PAPER

Analysis of DS-CDMA Transmission Performance in the Presence of Pure Impulsive Interference over Frequency Selective Fading

Eisuke KUDOH† *and* **Fumiyuki ADACHI**†, *Regular Members*

SUMMARY It is well known that some of urban man-made noises can be characterized by a wideband impulsive noise (pure impulsive noise). The presence of this pure impulsive noise may significantly degrade the wireless digital transmission performance. As the data rate becomes higher and the radio bandwidth becomes wider, the performance degradation due to pure impulsive interference may become larger. In this paper, the DS-CDMA transmission performance in the presence of pure impulsive interference is theoretically analyzed. First, the BER expressions are derived for DS-CDMA with antenna diversity and Rake combining in a frequency selective fading channel. Then, the numerical computation based on Monte-Carlo method is performed to evaluate the BER performance. Two types of error floor are observed: one is due to impulsive interference and the other due to the multi access interference (MAI). It is found that the error floor due to impulsive interference becomes larger as the area of impulse and the error floor is linearly proportional to the impulse occurrence rate. Furthermore, it is found that the antenna diversity and Rake combining do not help to reduce the error floor caused by impulsive interference and that the influence of impulsive interference can be negligible when the channel is limited by the MAI (i.e., large number of users are in communication).

key words: *impulsive interference, DS-CDMA, antenna diversity, Rake receiver*

1. Introduction

The man-made noise caused by vehicles, power lines, electrical equipments, etc, is a non-Gaussian random process. However, most practical receivers are designed to be optimal or near optimal against Gaussian noise. In mobile communications, a user may reach the vicinity of interference source where the impulsive interference may seriously degrade the signal transmission performance. Hence, the study of impulsive noise is of practical importance. As a statistical model of impulsive noise, the Middleton's class-A impulsive noise model [1] is well known. Another often used model is the ε-mixture model [3], [5], [11], which is the mixture of a heavy noise and a Gaussian distributed background noise. To obtain highly tractable performance results, the heavy noise is assumed as a Gaussian noise with large variance in [3], [5]. It is known [5], [11] that the ε-mixture model represents an approximation to the Middleton's class-A model. In the above models, impulsive interference is treated as a bandpass impulsive noise having narrower spectrum than the receiver bandwidth. On the other hand, ignition noise generated by internal combustion engines of vehicles can be characterized by a truly wideband impulsive noise [8]. Such noise can be modeled as a pure impulsive interference.

The influence of the bandpass impulsive interference on digital transmission performance has been studied extensively [1], [3], [5], [6], [11]. The bit error rate (BER) performance analysis of direct sequence code division multiple access (DS-CDMA) in the presence of the Middleton's class-A interference and the ε-mixture noise can be found in [6] and [5], respectively. Antenna diversity reception is a well-known technique to improve the BER performance in a multipath fading channel. The BER performance of TDMA with antenna diversity reception in the presence of the ε-mixture noise was theoretically analyzed in [3] to reveal that linear combining antenna diversity cannot effectively reduce the influence of impulsive interference. Theoretical analysis of the effect of pure impulsive interference on a narrowband digital system can be found in [9] and [10]. The performance degradation due to ignition interference (pure impulsive interference) was experimentally evaluated for a narrowband digital system to show that the impulsive interference significantly degrades the BER performance [2].

Recently, the radio bandwidth has become wider and wider to meet the demands for higher data rate transmissions. The third generation mobile communication systems use wideband DS-CDMA of around 5 MHz to increase the data rate with improved quality [4]. A pure impulsive interference may cause significant performance degradation in such a wideband system. Another cause of performance degradation in a wideband system is the frequency selective fading, which can be overcome by antenna diversity reception and Rake combining. To the best of authors' knowledge, the BER performance of DS-CDMA with antenna diversity and Rake combining in the presence of pure impulsive interference has not been fully understood.

Motivated by the above, assuming pure impulsive interference, this paper analyzes the BER performance of DS-CDMA with antenna diversity and Rake com-

Manuscript received February 5, 2002.
Manuscript revised May 2, 2002.

†The authors are with Electrical and Communication Engineering, Graduate School of Engineering, Tohoku University, Sendai-shi, 980-8579 Japan.

bining in frequency selective fading. In Sect. 2, BER expressions are derived. Then, in Sect. 3, the numerical computation based on Monte-Carlo method is performed to evaluate the BER performance for the single user case and the multi-user case. Sect. 4 draws some conclusions.

2. Derivation of BER Expression in the Presence of Impulsive Interference

2.1 Transmission System Model

M-branch antenna diversity reception is considered. Figure 1 illustrates the antenna arrangement and Fig. 2 shows the DS-CDMA receiver structure. Quadrature phase shift keying (QPSK) and binary PSK (BPSK) are assumed for data modulation and spreading modulation, respectively. K users are assumed to be in simultaneous communication. The propagation channel is assumed to have L discrete paths having different time delays and independent Rayleigh fading. It is assumed that the source of impulsive interference is located in line of sight, but, sufficiently far from the receiver of interest and hence it arrives as a plane wave with the same incident angle to all the receiver antennas. The received signal on each antenna is the sum of spread signals of different users, the impulsive interference, and the background noise. An ideal L-finger coherent Rake combiner based on maximal ratio combining (MRC) is assumed. In each Rake finger, the composite signal is de-spread by a correlator whose timing is synchronized to each propagation path, and multiplied by the complex conjugate of channel gain of the corresponding path. All finger outputs of M antennas are then combined.

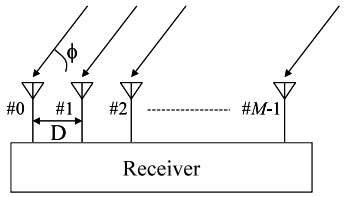

Fig. 1 Antenna arrangement.

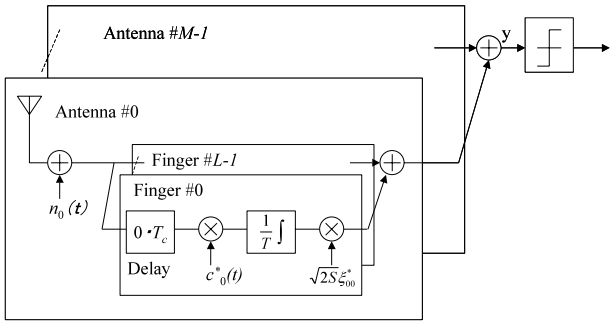

Fig. 2 DS-CDMA receiver structure.

2.2 Received Signal

Since we are interesting in the theoretical analysis of the impulsive interference effect, ideal linear amplifier is assumed (note that the use of a limiter receiver can improve the BER performance in the presence of impulsive interference [6]). The received signal $r_m(t)$ on the mth antenna is expressed using the equivalent baseband representation as

$$r_m(t) = \sqrt{2S} \sum_{q=-\infty}^{\infty} \sum_{k=0}^{K-1} \sum_{l=0}^{L-1} \xi_{k,m,l}(q) d_k(q) \cdot c_k(t - qT - lT_c) + I_m(t) + n_m(t), \quad (1)$$

where S is the average received signal power, $\xi_{k,m,l}(q)$ is the complex Gaussian process representing the channel gain of the lth path seen on the mth antenna of the kth user's receiver, and $d_k(q)$ is the qth data symbol of kth user. It has been assumed that the time delays of L paths are chip spaced (i.e., T_c) and the channel gain remains constant over one symbol duration T. Note that $T = (SF)T_c = 2(PG)T_c$ for QPSK data modulation, where SF is the spreading factor defined as the number of chips per data symbol, PG is the processing gain defined as the number of chips per data bit. $c_k(t)$ is the kth user's spreading chip waveform and is represented as

$$c_k(t) = \sum_{i=-\infty}^{\infty} c_{k,i} u(t - iT_c), \quad (2)$$

where

$$c_{k,i} \in (1, -1)$$
$$u(t) = \begin{cases} 1, & 0 \le t < T_c \\ 0, & \text{elsewhere} \end{cases} \quad (3)$$

where $\{c_{k,i}\}$ is the random spreading code sequence. Note that for the forward (base-to-mobile) link, $\{c_{k,i}\}$'s are generated by multiplying SF-length orthogonal sequences by a long pseudo noise (PN) random sequence which is different for different base stations. The reverse (mobile-to-base) link is asynchronous while the forward link is synchronous, but in this paper, synchronous link is assumed for the simplicity of analysis (the reverse link applies different long PN spreading sequences to different users and thus, the assumption of synchronous timing does not cause any difference). In Eq. (1), $I_m(t)$ and $n_m(t)$ represent the received impulsive interference and the additive white Gaussian noise (AWGN) with one-sided power spectrum density N_0. $I_m(t)$ may be expressed as

$$I_m(t) = I(t) \exp[j2m\pi(D/\lambda)\cos\phi], \quad (4)$$

where ϕ is the incident angle to antennas, λ is the carrier wavelength, D is the antenna separation, and

$$I(t) = A\sum_{n}\delta(t-t_n) \tag{5}$$

with t_n being the occurrence time of the nth impulse.

2.3 Rake Combiner Output

First, we consider the reverse link. In each Rake finger, the received signal is correlated with the spreading waveform $c_k(t)$. The 0th data symbol of the 0th user ($k=q=0$ in Eq. (1)) is to be detected. Assuming that one impulse has occurred at the nth chip timing of the first arrival path (i.e., zero time delay), the lth finger output may be expressed as

$$\begin{aligned} y_{m,l} =\ & \sqrt{2S}\xi_{0,m,l}d_0 + \tilde{I}_{m,l} \\ & + \frac{1}{T}\sum_{\substack{l'=0\\ l'\neq l}}^{L-1}\sqrt{2S}\xi_{0,m,l'}\int_0^T d_0 c_0(t-l'T_c) \\ & \cdot c_0^*(t-lT_c)dt \\ & + \frac{1}{T}\sum_{l'=0}^{L-1}\sum_{k=1}^{K-1}\sqrt{2S}\xi_{k,m,l'}\int_0^T d_k c_k(t-l'T_c) \\ & \cdot c_0^*(t-lT_c)dt \\ & + \frac{1}{T}\int_0^T n_m(t-lT_c)c_0^*(t-lT_c)dt, \end{aligned} \tag{6}$$

where $\xi_{k,m,l} = \xi_{k,m,l}(0)$ and $d_k = d_k(0)$ for simplicity, and

$$\begin{aligned} \tilde{I}_{m,l} &= \frac{1}{T}\int_0^T I_m(t)c_0^*(t-lT_c)dt \\ &= \frac{A}{T}c_{0,n-l}^*\exp\left[j2m\pi\frac{D}{\lambda}\cos\phi\right], \end{aligned} \tag{7}$$

is the contribution from the impulsive interference to the lth Rake finger output. We are assuming a pure impulsive interference model [9], [10] as presented in Eq. (5). The pure impulse has the infinite amplitude, resulting in infinite power. However, since the despreading process is equivalent to an integration filter with the bandwidth of $1/T$, the band-limited impulsive interference has the finite amplitude, which is A/T as understood from Eq. (7).

The desired signal components in the L finger outputs are coherently combined by the Rake combiner based on MRC. Hence, the Rake combiner output $y_{reverse}$ is represented as

$$\begin{aligned} & y_{reverse} \\ &= \sqrt{2S}\sum_{m=0}^{M-1}\sum_{l=0}^{L-1} y_{m,l}\xi_{0,m,l}^* \\ &= 2Sd_0\sum_{m=0}^{M-1}\sum_{l=0}^{L-1}|\xi_{0,m,l}|^2 \\ &\quad + \frac{\sqrt{2S}A}{T}\sum_{m=0}^{M-1}\sum_{l=0}^{L-1}\xi_{0,m,l}^* c_{0,n-l}^*\exp\left[j2\pi m\frac{D}{\lambda}\cos\phi\right] \\ &\quad + \frac{2S}{T}\sum_{m=0}^{M-1}\sum_{l=0}^{L-1}\sum_{\substack{l'=0\\ l'\neq l}}^{L-1}\xi_{0,m,l'}\xi_{0,m,l}^* d_0 \\ &\quad \cdot\int_0^T c_0(t-l'T_c)c_0^*(t-lT_c)dt \\ &\quad + \frac{2S}{T}\sum_{m=0}^{M-1}\sum_{l=0}^{L-1}\sum_{l'=0}^{L-1}\sum_{k=1}^{K-1}\xi_{k,m,l'}\xi_{0,m,l}^* d_k \\ &\quad \cdot\int_0^T c_k(t-l'T_c)c_0^*(t-lT_c)dt \\ &\quad + \frac{\sqrt{2S}}{T}\sum_{m=0}^{M-1}\sum_{l=0}^{L-1}\xi_{0,m,l}^*\int_0^T n_m(t-lT_c)c_0^*(t-lT_c)dt, \end{aligned} \tag{8}$$

which is the decision variable. The first term is the desired signal component, the second term the contribution from the impulse, the third term the inter-path interference (IPI) from own user, the forth term the MAI, and the last term the noise component due to AWGN.

Rake fingers are time-synchronized to the time delays of the multipath channel. Because of this, the relative time positions of the impulsive interference seen on the different Rake fingers become different. Therefore, it is interesting to note that the impulsive interference is transformed to a chain of L impulses having time delays same to those of the propagation channel.

Next, the forward link is considered. Unlike the reverse link, the forward link is synchronous and the orthogonal spreading codes can be used so that MAI is not produced in the same path. Furthermore, transmitted spread signals from all users experience the same fading, i.e., $\xi_{k,m,l} = \xi_{0,m,l}$. Hence, the Rake combiner output $y_{forward}$ is represented as

$$\begin{aligned} & y_{forward} \\ &= \sqrt{2S}\sum_{m=0}^{M-1}\sum_{l=0}^{L-1} y_{m,l}\xi_{0,m,l}^* \\ &= 2Sd_0\sum_{m=0}^{M-1}\sum_{l=0}^{L-1}|\xi_{0,m,l}|^2 \\ &\quad + \frac{\sqrt{2S}A}{T}\sum_{m=0}^{M-1}\sum_{l=0}^{L-1}\xi_{0,m,l}^* c_{0,n-l}^*\exp\left[j2\pi m\frac{D}{\lambda}\cos\phi\right] \\ &\quad + \frac{2S}{T}\sum_{m=0}^{M-1}\sum_{l=0}^{L-1}\sum_{\substack{l'=0\\ l'\neq l}}^{L-1}\xi_{0,m,l'}\xi_{0,m,l}^* d_0 \\ &\quad \cdot\int_0^T c_0(t-l'T_c)c_0^*(t-lT_c)dt \end{aligned}$$

$$+\frac{2S}{T}\sum_{m=0}^{M-1}\sum_{l=0}^{L-1}\sum_{\substack{l'=0\\ l'\neq l}}^{L-1}\xi_{0,m,l'}\xi_{0,m,l}^{*}$$
$$\cdot\sum_{k=1}^{K-1}d_k\int_0^T c_k(t-l'T_c)c_0^{*}(t-lT_c)dt$$
$$+\frac{\sqrt{2S}}{T}\sum_{m=0}^{M-1}\sum_{l=0}^{L-1}\xi_{0,m,l}^{*}\int_0^T n_m(t-lT_c)c_0^{*}(t-lT_c)dt. \tag{9}$$

2.4 BER Expression

Assuming that the four phase symbols of QPSK are transmitted equally likely, transmission of $d_0=(1+j)/\sqrt{2}$ (representing (1, 1) transmission) is considered without loss of generality. The conditional error probability of the first bit for the given $\{\xi_{k,m,l};\ k=0\sim K-1,\ m=0\sim M-1,\ l=0\sim L-1\}$ and $\{d_k;\ k=0\sim K-1\}$ can be obtained once the statistical properties of $\mathrm{Re}[y]|\{\xi_{k,m,l},\ d_0=(1+j)/\sqrt{2},\ d_k\}$ are known.

First, we consider the reverse link. From Eq. (8), $\mathrm{Re}[y_{reverse}]|\{\xi_{k,m,l},\ d_0=(1+j)/\sqrt{2},\ d_k\}$ is given by

$$\begin{aligned}
&\mathrm{Re}[y_{reverse}]|\{\xi_{k,m,l},\ d_0=(1+j)/\sqrt{2},\ d_k\}\\
&\quad=\sqrt{2}S\sum_{m=0}^{M-1}\sum_{l=0}^{L-1}|\xi_{0,m,l}|^2+\frac{\sqrt{2S}A}{T}\sum_{m=0}^{M-1}\sum_{l=0}^{L-1}\\
&\qquad\cdot\mathrm{Re}[\xi_{0,m,l}^{*}c_{0,n-l}^{*}\exp\{j2\pi m(D/\lambda)\cos\phi\}]\\
&\qquad+\frac{2S}{T}\sum_{m=0}^{M-1}\sum_{l=0}^{L-1}\sum_{\substack{l'=0\\ l'\neq l}}^{L-1}\mathrm{Re}[\xi_{0,m,l'}\xi_{0,m,l}^{*}d_0]\\
&\qquad\cdot\int_0^T c_0(t-l'T_c)c_0(t-lT_c)dt\\
&\qquad+\frac{2S}{T}\sum_{m=0}^{M-1}\sum_{l=0}^{L-1}\sum_{l'=0}^{L-1}\sum_{k=1}^{K-1}\mathrm{Re}[\xi_{k,m,l'}\xi_{0,m,l}^{*}d_k]\\
&\qquad\cdot\int_0^T c_k(t-l'T_c)c_0(t-lT_c)dt\\
&\qquad+\frac{\sqrt{2S}}{T}\sum_{m=0}^{M-1}\sum_{l=0}^{L-1}\\
&\qquad\mathrm{Re}\left[\xi_{0,m,l}^{*}\int_0^T n_m(t-lT_c)c_0^{*}(t-lT_c)dt\right].
\end{aligned}\tag{10}$$

By observing Eq. (10), it is understood that the incident angle ϕ of impulsive interference has no impact on the average decision error, since the channel gain is a complex Gaussian variable and its phase is uniformly distributed over $[-\pi,\pi]$. Therefore, $\exp[j2\pi m(D/\lambda)\cos\phi]$ can be dropped from the second term of Eq. (10). The integral $\int_0^T c_k(t-l'T_c)c_0^{*}(t-lT_c)dt$ in the third term has a zero mean binomial distribution and can be well approximated as a zero mean Gaussian variable for large PG from the central limit theorem. Since there are $2PG$ chips in one QPSK symbol period T, its variance is given by $T^2/(2PG)$. The integral $\int_0^T n_m(t-lT_c)c_0^{*}(t-lT_c)dt$ in the noise component due to AWGN is a complex Gaussian variable of zero mean and variance $2N_0T$. Taking into account the above, $\mathrm{Re}[y_{reverse}]|\{\xi_{k,m,l},\ d_0=(1+j)/\sqrt{2},\ d_k\}$ is approximated as a Gaussian variable with average m_0 and variance σ_0^2:

$$\begin{cases}
m_0=\sqrt{2}S\displaystyle\sum_{m=0}^{M-1}\sum_{l=0}^{L-1}|\xi_{0,m,l}|^2\\
\qquad+\dfrac{\sqrt{2S}\cdot A}{T}\displaystyle\sum_{m=0}^{M-1}\sum_{l=0}^{L-1}\mathrm{Re}[\xi_{0,m,l}]\\
\sigma_0^2=\dfrac{2S^2}{PG}\displaystyle\sum_{m=0}^{M-1}\sum_{l=0}^{L-1}\sum_{\substack{l'=0\\ l'\neq l}}^{L-1}\mathrm{Re}^2[\xi_{0,m,l'}\xi_{0,m,l}^{*}d_0]\\
\qquad+\dfrac{2S^2}{PG}\displaystyle\sum_{m=0}^{M-1}\sum_{l=0}^{L-1}\sum_{l'=0}^{L-1}\sum_{k=1}^{K-1}\mathrm{Re}^2[\xi_{k,m,l'}\xi_{0,m,l}^{*}d_k]\\
\qquad+\dfrac{2SN_0}{T}\displaystyle\sum_{m=0}^{M-1}\sum_{l=0}^{L-1}|\xi_{0,m,l}|^2.
\end{cases}\tag{11}$$

Then, the conditional error probability is obtained as

$$\begin{aligned}
&\Pr(\mathrm{Re}[y_{reverse}]<0|\{\xi_{k,m,l},\ d_0=(1+j)/\sqrt{2},d_k\})\\
&\quad=\frac{1}{2}\mathrm{erfc}\left(\frac{m_0}{\sqrt{2}\sigma_0}\right)=\frac{1}{2}\mathrm{erfc}(X\sqrt{Y}),
\end{aligned}\tag{12a}$$

with

$$X=1+\frac{\dfrac{A}{\sqrt{2N_0}}\dfrac{1}{\sqrt{T}}\displaystyle\sum_{m=0}^{M-1}\sum_{l=0}^{L-1}\mathrm{Re}[\xi_{0,m,l}]}{\sqrt{\left(\dfrac{E_b}{N_0}\right)}\displaystyle\sum_{m=0}^{M-1}\sum_{l=0}^{L-1}|\xi_{0,m,l}|^2}$$

$$Y=\frac{\left(\dfrac{E_b}{N_0}\right)\displaystyle\sum_{m=0}^{M-1}\sum_{l=0}^{L-1}|\xi_{0,m,l}|^2}{1+\dfrac{2}{PG}\left(\dfrac{E_b}{N_0}\right)\dfrac{\left(\begin{array}{l}\displaystyle\sum_{m=0}^{M-1}\sum_{l=0}^{L-1}\sum_{\substack{l'=0\\ l'\neq l}}^{L-1}\\ \mathrm{Re}^2[\xi_{0,m,l'}\xi_{0,m,l}^{*}d_0]\\ \quad+\displaystyle\sum_{m=0}^{M-1}\sum_{l=0}^{L-1}\sum_{l'=0}^{L-1}\sum_{k=0}^{K-1}\\ \mathrm{Re}^2[\xi_{k,m,l'}\xi_{0,m,l}^{*}d_k]\end{array}\right)}{\displaystyle\sum_{m=0}^{M-1}\sum_{l=0}^{L-1}|\xi_{0,m,l}|^2}}$$

(12b)

where $\mathrm{erfc}(x) = (2/\sqrt{\pi})\int_x^\infty \exp(-t^2)dt$ and E_b ($= ST/2$) is the received signal energy per bit.

Similarly, the conditional error probability for the forward link is obtained as

$$\Pr(\mathrm{Re}[y_{forward}] < 0 \,|\, \{\xi_{0,m,l}, d_0 = (1+j)/\sqrt{2}, d_k\}|) = \frac{1}{2}\mathrm{erfc}(X\sqrt{Y}) \tag{13a}$$

with

$$X = 1 + \frac{\dfrac{A}{\sqrt{2N_0}}\dfrac{1}{\sqrt{T}}\displaystyle\sum_{m=0}^{M-1}\sum_{l=0}^{L-1}\mathrm{Re}[\xi_{0,m,l}]}{\sqrt{\dfrac{E_b}{N_0}}\displaystyle\sum_{m=0}^{M-1}\sum_{l=0}^{L-1}|\xi_{0,m,l}|^2}$$

$$Y = \frac{\left(\dfrac{E_b}{N_0}\right)\displaystyle\sum_{m=0}^{M-1}\sum_{l=0}^{L-1}|\xi_{0,m,l}|^2}{\displaystyle\sum_{m=0}^{M-1}\sum_{l=0}^{L-1}\sum_{\substack{l'=0\\ l'\neq l}}^{L-1}\sum_{k=0}^{K-1}} 1 + \frac{2}{PG}\left(\frac{E_b}{N_0}\right)\frac{\mathrm{Re}^2[\xi_{0,m,l}\xi^*_{0,m,l'}d_k]}{\displaystyle\sum_{m=0}^{M-1}\sum_{l=0}^{L-1}|\xi_{0,m,l}|^2} \tag{13b}$$

Finally, the average BERs $P_b(A)$'s of the reverse link and the forward link in the presence of impulsive interference can be computed by averaging Eqs. (12) and (13), respectively, over $\{\xi_{k,m,l}\}$ and $\{d_k\}$:

$$\begin{aligned} P_b(A) &= \Pr(\mathrm{Re}[y] < 0 \mid d_0 = (1+j)/\sqrt{2}) \\ &= \int\cdots\int \Pr(\mathrm{Re}[y] < 0 \mid \{\xi_{k,m,l}, \\ &\quad d_0 = (1+j)/\sqrt{2}, d_k\}) \\ &\quad \times \prod_{k,m,l}\{p(\xi_{k,m,l})d\xi_{k,m,l}\} \times \prod_k \{p(d_k)dd_k\}. \end{aligned} \tag{14}$$

Assuming that the interference source does not generate more than one impulse in one data symbol period, the overall BER P_b is given by

$$P_b = P_{pulse}P_b(A) + (1 - P_{pulse})P_b(A = 0), \tag{15}$$

where $P_b(A = 0)$ is the average BER in the presence of no impulsive interference and P_{pulse} is the probability of the occurrence of the impulse per data symbol (or the impulse occurrence rate normalized by QPSK data symbol rate).

It can be understood from Eqs. (12), (13) and (15) that the influence of impulsive noise on the BER performance is governed by the following parameters: the normalized impulse area $A/\sqrt{2N_0}$, the symbol rate T, and the impulse occurrence rate P_{pulse}.

3. Numerical Results

The bit errors are produced by AWGN and MAI as well as impulsive interference. For the multipath channel, the uniform power delay profile is assumed, i.e., $E[|\xi_{k,m,l}|^2] = 1/L$ for all k and m, where E[.] represents ensemble average. Unless otherwise stated, it is assumed that the spreading chip rate is 32 MHz, the symbol rate is 1 Msymbol/s (sps) (i.e., $T = 10^{-6}$ sec and $PG = 32$), $P_{pulse} = 10^{-3}$, $L = 4$, and $M = 4$.

The average BER $P_b(A)$ in the presence of impulsive interference is given by Eq. (14). However, obtaining the closed-form equation is very difficult if not impossible. Therefore, we apply the Monte Carlo simulation to numerically compute Eq. (14). The multiple-integration required in Eq. (14) is performed based on Monte Carlo method. Since $\mathrm{Re}[y_{reverse}]|\{\xi_{k,m,l},\ d_0 = (1+j)/\sqrt{2}, d_k\}$ in Eq. (14) can be approximated as a Gaussian distribution, the conditional error probability for the given $\{\xi_{k,m,l};\ k = 0 \sim K-1,\ m = 0 \sim M-1,\ l = 0 \sim L-1\}$ and $\{d_k;\ k = 0 \sim K-1\}$ can be expressed using the complimentary error function. Numerical computation of $P_b(A)$ based on Monte Carlo method is performed as follows. First, the set of independent channel gains $\{\xi_{k,m,l}\}$ and QPSK symbols $\{d_k\}$ are generated. Then, using Eqs. (12) and (13), the conditional error probability is computed. This is repeated 1 million times to obtain $P_b(A)$.

3.1 Effects of $A/\sqrt{2N_0}$, $1/T$, and P_{pulse}

To begin with, the single user case ($K = 1$) is assumed. It is understood from Eqs. (12) and (13) that the BER performance of reverse link is identical to that of forward link. How $A/\sqrt{2N_0}$, $1/T$, and P_{pulse} affect the BER performance is discussed assuming the constant chip rate of 64 Mchip/s (i.e., the spreading bandwidth of 64 MHz). The computed results are plotted in Figs. 3–5.

Figure 3 plots the $P_b(A)$ curves with $A/\sqrt{2N_0}$ as parameter assuming $M = L = 1$. The BER performance with $A/\sqrt{2N_0} = 0.0001$ was found to be almost identical to that in the presence of no impulsive interference. Increasing the value of $A/\sqrt{2N_0}$ degrades the BER performance. When the impulse becomes stronger by 20 dB, the BER performance curve is shifted towards right by 20 dB.

The relationship between the desired signal rms amplitude and the area of impulsive interference is discussed below. The instantaneous rms amplitude of desired signal after despreading is given by $\sqrt{S}|\xi| = \sqrt{2E_b/T}|\xi|$ from Eq. (6), where the signal energy per bit $E_b = ST/2$ for QPSK data modulation and ξ denotes the complex channel gain characterized by a complex Gaussian process. For simplicity, we have assumed a one-path propagation channel, single antenna

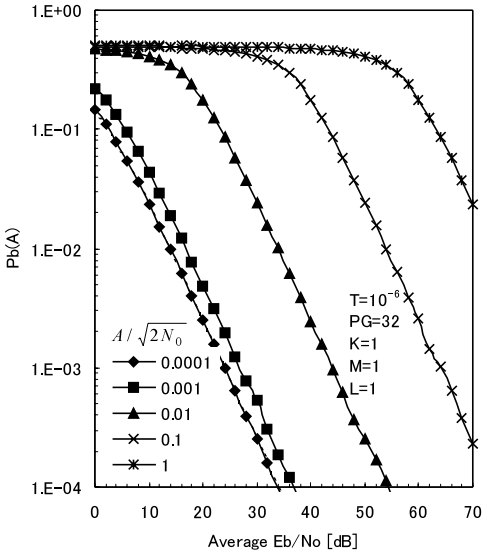

Fig. 3 Effect of $A/\sqrt{2N_0}$ on $P_b(A)$. Single-user case.

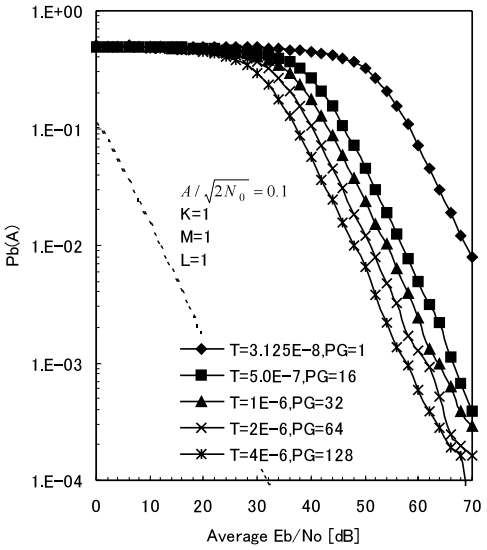

Fig. 4 Effect of symbol rate on $P_b(A)$. Single-user case.

reception and the single user, i.e., $M = L = K = 1$. On the other hand, the amplitude of impulsive interference after despreading becomes A/T as seen from Eq. (7). Consequently, the instantaneous desired signal rms amplitude-to-impulsive interference amplitude ratio χ after despreading becomes

$$\chi = \frac{\sqrt{S}}{A/T}|\xi| = \left(\sqrt{\frac{E_b}{N_0}}\frac{\sqrt{T}}{A/\sqrt{2N_0}}\right)|\xi| = \alpha|\xi|. \quad (16)$$

For example, if the average signal energy per bit-to-AWGN power spectrum density ratio (average E_b/N_0) $= 30\,\mathrm{dB}$, $A/\sqrt{2N_0} = 0.01$ and $T = 10^{-6}$ [sec], the value of α is $\sqrt{10}$. However, it should be noted that $|\xi|$ is a Rayleigh distributed random variable with $E[|\xi|^2] = 1$. The probability density function (pdf) of χ is given by

$$p(\chi) = \frac{\chi}{\alpha^2}\exp\left(-\frac{\chi^2}{2\alpha^2}\right). \quad (17)$$

Assuming that bit errors are produced at the probability of almost 1/2 when $\chi \le 1$, $P_b(A)$ can be approximately computed from

$$P_b(A) \approx \frac{1}{2}\int_0^1 p(\chi)d\chi = \frac{1}{2}\left[1 - \exp\left(-\frac{1}{2\alpha^2}\right)\right]. \quad (18)$$

When the average $E_b/N_0 = 30\,\mathrm{dB}$ and $A/\sqrt{2N_0} = 0.01$, the approximate $P_b(A)$ computed from Eq. (18) becomes $P_b(A) \approx 2.4\times10^{-2}$, which agrees quite well with the result presented in Fig. 3.

Figure 4 plots the $P_b(A)$ curves with the symbol rate as parameter. The range of the symbol rates is from 0.25 Msps to 32 Msps (i.e., $PG = 128$ to 1). For comparison, the BER performance curve in the presence of no impulsive interference is plotted as a dotted line. For the given chip rate, the BER performance degrades as the symbol rate increases. Two times increase in the symbol rate degrades the BER performance by about 3.5 dB.

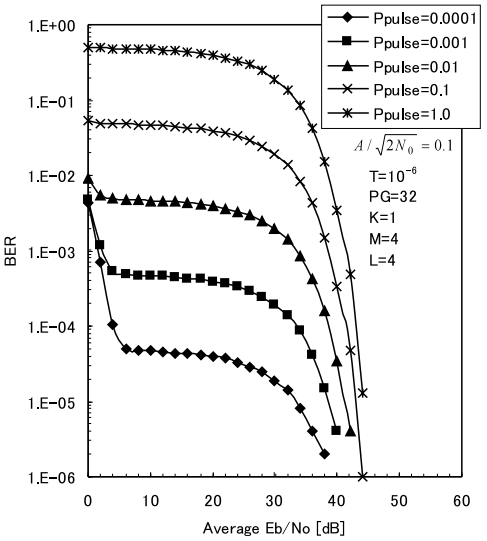

Fig. 5 Effect of P_{pulse} on overall BER performance. Single-user case.

Figure 5 plots the overall BER performance curves with P_{pulse} as a parameter for $M = L = 4$. As the average E_b/N_0 increases, the BER falls first and remains almost constant (BER floor) until a certain average E_b/N_0 value, beyond which the BER value starts to fall again. The BER floor value is determined by the impulse occurrence rate P_{pulse} while the BER floor region is determined by the value of $A/\sqrt{2N_0}$ and T as can be understood from Figs. 3 and 4. In the BER floor region, the impulsive interference is a predominant cause of errors and hence, from Eq. (15), P_b is approxi-

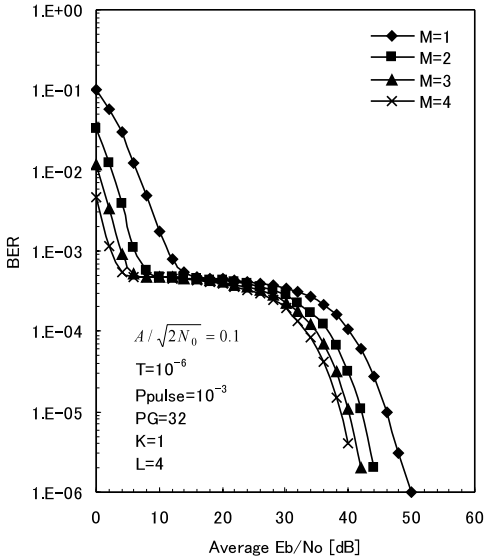

Fig. 6 Effect of antenna diversity on overall BER performance. Single-user case.

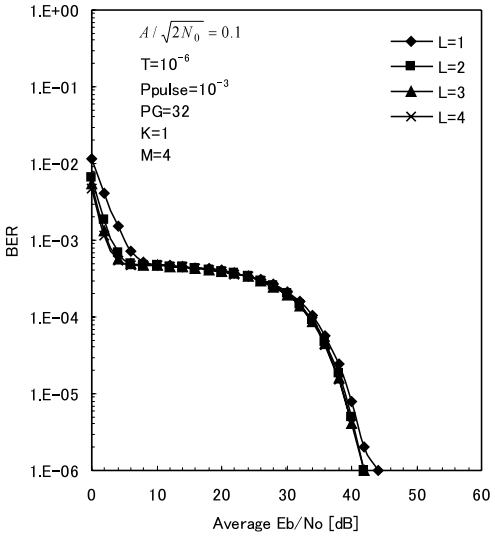

Fig. 7 Effect of Rake combining on overall BER performance. Single-user case.

mately given by $P_b \cong P_b(A)P_{pulse}$. Therefore, the BER floor value is in proportion to P_{pulse}.

3.2 Effects of Antenna Diversity and Rake Combining

Again here, the single user case ($K = 1$) is assumed. Figure 6 shows how antenna diversity improves the BER performance assuming an $L = 4$-finger Rake combining. It is seen in Fig. 6 that antenna diversity does not help to reduce the BER floor due to impulsive interference at all as found in [3]. In this region, the probability $P_b(A)$ of error due to impulsive interference is almost 0.5 since the impulsive interference is much stronger than the desired signal. Hence, such error cannot be eliminated by antenna diversity reception.

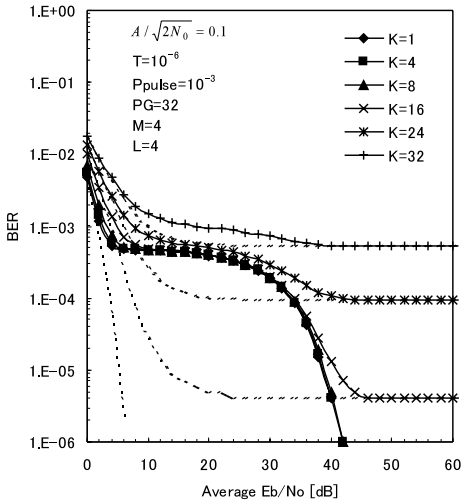

(a) Forward link

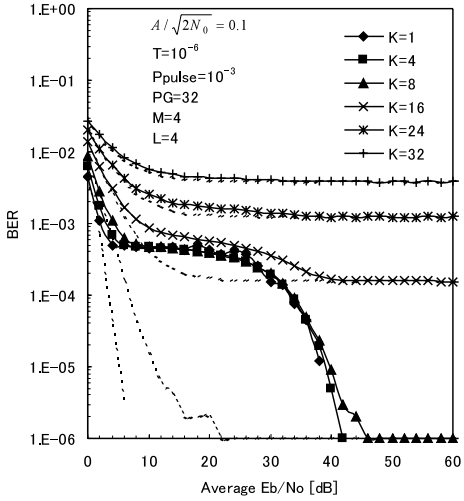

(b) Reverse link

Fig. 8 Effect of number K of users on overall BER performance. Multi-user case.

Figure 7 shows how the Rake combining improves the BER performance for $L = 1 \sim 4$. As found for antenna diversity reception, Rake combining effect is not helpful to reduce the influence of impulsive interference. This is due to the fact that the decision error is produced with a probability of almost 0.5 when strong impulse occurs.

3.3 BER Performance in Multi-User Case

So far we have considered the single user case. Here, we extend the evaluation to the multi-user case. The BER floor is produced by MAI in addition to impulsive noise. It is interesting to see how differently the impulsive interference impacts the overall BER performances of the reverse link and forward link. Figure 8 plots the BER performance with the number K of users as a

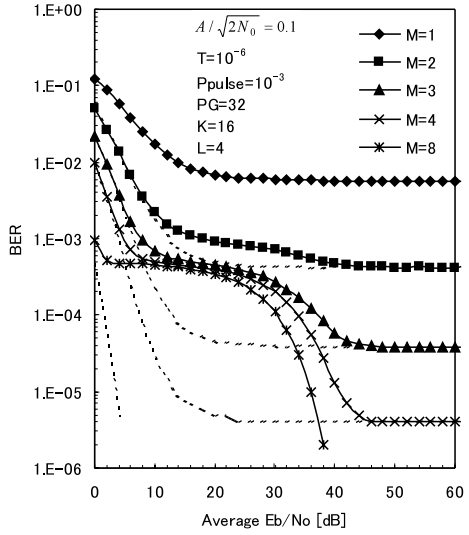

(a) Forward link

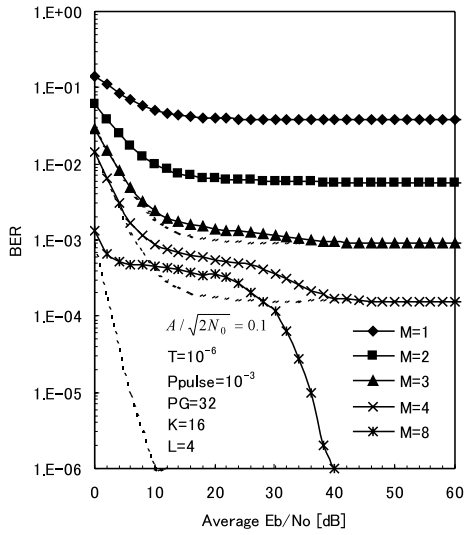

(b) Reverse link

Fig. 9 Effect of antenna diversity on overall BER performance. Multi-user case.

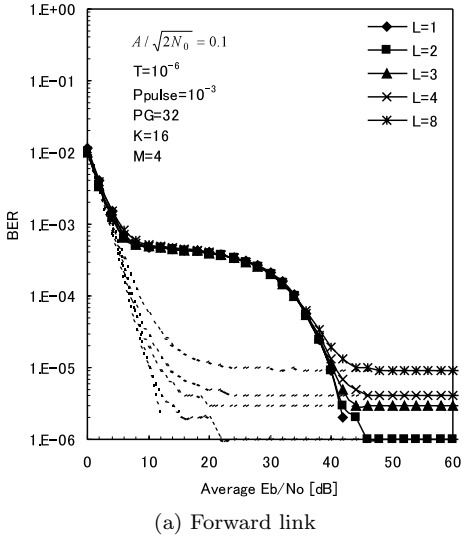

(a) Forward link

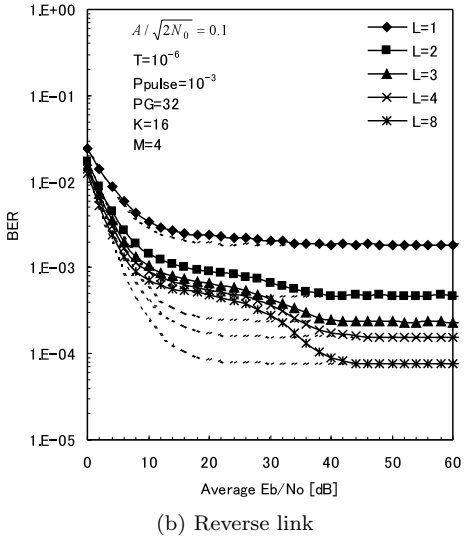

(b) Reverse link

Fig. 10 Effect of Rake combing on overall BER performance. Multi-user case.

parameter. For comparison, the BER performances in the presence of no impulsive interference are plotted as dotted lines. As K increases, the influence of impulsive interference tends to be masked by MAI when $K > 16$ (i.e., $K/PG = 0.5$) on the reverse link but $K > 24$ (i.e., $K/PG = 0.75$) on the forward link (this is because of smaller MAI on the forward link owing to orthogonal spreading codes).

Figure 9 plots the BER performance with the number M of antenna as a parameter for $L = 4$ and $K = 16$ (i.e., $K/PG = 0.5$). For comparison, the BER performance in the presence of no impulsive interference is also plotted as dotted lines. Without antenna diversity, the BER performance is almost governed by MAI. The BER due to MAI reduces as M increases. However, as mentioned earlier, antenna diversity has no effect in reducing the BER produced by impulsive interference and hence, the error floor starts to appear when M increases to 3 (4) on the forward (reverse) link. It should be noticed that the BER floor due to impulsive noise is the same for both reverse and forward links.

Figure 10 plots the BER performance with the number L of Rake fingers as parameter for $M = 4$ and $K = 16$ (i.e., $K/PG = 0.5$). For comparison, the BER performances in the presence of no impulsive interference are plotted as dotted lines. For the forward link, the performance improvement against MAI is already saturated with an $M = 4$-antenna diversity reception and hence, no additional performance improvement can be obtained by Rake combining. Hence, the BER floor due to impulsive noise is visible. However, on the reverse link, the MAI still remains predominant even with an $M = 4$-antenna diversity reception. Hence, Rake combining can improve the BER performance. But

when L is more than 3, the BER floor region due to impulsive interference exists.

4. Conclusions

BER expressions for DS-CDMA with antenna diversity and Rake combining in the presence of pure impulsive interference were derived and then, the BER performance was computed based on Monte-Carlo method. The impact of the pure impulsive interference on the BER performance was discussed. The results obtained in this paper can be summarized as follows:

(a) The incident angle ϕ of impulsive interference to diversity antennas has no impact on the average decision error.
(b) Impulsive interference produces BER floor. The BER floor value is governed by the impulse occurrence rate P_{pulse} while the BER floor region is determined by the value of $A/\sqrt{2N_0}$ and T.
(c) Antenna diversity reception and Rake combining do not help to reduce the BER floor produced by impulsive interference. They are however effective in reducing the BER floor due to MAI.

The results obtained in this paper can be used to estimate the performance degradation in the presence of pure impulsive interference. The assumption made in this paper on the pure impulsive interference was that the impulses always have the same area A. However, in a real environment, the value of A may be a random variable and impulses may arrive in groups. How these affect the BER performance is left for future study. Also, an interesting extension of the analysis is to the case of Middleton's class A impulsive noise model.

References

[1] D. Middleton, "Statistical-physical models of electromagnetic interference," IEEE Trans. Electromagn. Compat., vol.19, no.3, pp.106–127, Aug. 1997.
[2] S. Nakamura, "A study of errors caused by impulsive noise and a simple estimation method for digital mobile communications," IEEE Trans. Veh. Technol., vol.45, no.2, pp.310–317, May 1996.
[3] R.S. Blum, R.J. Kozick, and B.M. Sadler, "An adaptive spatial diversity receiver for non-Gaussian interference and noise," IEEE Trans. Signal Processing, vol.47, no.8, pp.2100–2111, Aug. 1999.
[4] F. Adachi, M. Sawahashi, and H. Suda, "Wideband DS-CDMA for next-generation mobile communications systems," IEEE Commun. Mag., vol.36, pp.56–69, Sept. 1998.
[5] B. Aazhang and H.V. Poor, "Performance of DS/SSMA communications in impulsive channels—Part I: Linear correlation receivers," IEEE Trans. Commun., vol.COM-35, no.11, pp.1179–1188, Nov. 1987.
[6] S. Unawong, S. Miyamoto, and N. Morinaga, "A novel receiver design for DS-CDMA systems under impulsive radio noise environments," IEICE Trans. Commun., vol.E82-B, no.6, pp.936–943, June 1999.
[7] F. Adachi, "Effects of orthogonal spreading and Rake combining on DS-CDMA forward link in mobile radio," IEICE Trans. Commun., vol.E80-B, no.11, pp.1703–1712, Nov. 1997.
[8] H.S. Oranc, "Ignition noise measurements in the VHF/UHF bands," IEEE Trans. Electromagn. Compat., vol.EMC-17, no.2, pp.54–64, May 1975.
[9] P.A. Bello and R. Esposito, "A new method for calculationg probabilities of errors due to impulsive noise," IEEE Trans. Commun., vol.COM-17, no.3, pp.368–379, June 1969.
[10] M.M. Pejanovic, J.A. Edwards, and I.S. Stojanovic, "Error rate prediction for NCFSK digital mobile radio system," IEE Proceedings, vol.134, no.1, pp.21–26, Feb. 1987.
[11] K.S. Vastola, "Threshold detection in narrow-band non-Gaussian noise," IEEE Trans. Commun., vol.COM-32, no.2, pp.134–139, Feb. 1984.

Eisuke Kudoh received the B.S. and M.S. degrees in physics and Ph.D. degree in electronic engineering from Tohoku University, Sendai, Japan, in 1986, 1988, and 2001, respectively. In April 1988, he joined the NTT Radio Communication Systems Laboratories, Kanagawa, Japan. He was engaged in research on digital mobile and personal communication systems including CDMA systems and error control schemes, etc. Since October 2001, he has been with Tohoku University, Sendai, Japan, where he is an Associate Professor of Electrical and Communication Engineering at Graduate School of Engineering. His research interests are in wireless network, wireless packet transmission, etc.

Fumiyuki Adachi received his B.S. and Dr.Eng. degrees in electrical engineering from Tohoku University, Sendai, Japan, in 1973 and 1984, respectively. In April 1973, he joined the Electrical Communications Laboratories of Nippon Telegraph & Telephone Corporation (now NTT) and conducted various types of research related to digital cellular mobile communications. From July 1992 to December 1999, he was with NTT Mobile Communications Network, Inc. (now NTT DoCoMo, Inc.), where he led a research group on wideband/broadband CDMA wireless access for IMT-2000 and beyond. Since January 2000, he has been with Tohoku University, Sendai, Japan, where he is a Professor of Electrical and Communication Engineering at Graduate School of Engineering. His research interests are in CDMA and TDMA wireless access techniques, CDMA spreading code design, Rake receiver, transmit/receive antenna diversity, adaptive antenna array, bandwidth-efficient digital modulation, and channel coding, with particular application to broadband wireless communications systems. From October 1984 to September 1985, he was a United Kingdom SERC Visiting Research Fellow in the Department of Electrical Engineering and Electronics at Liverpool University. From April 1997 to March 2000, he was a visiting Professor at Nara Institute of Science and Technology, Japan. He has written chapters of three books: Y. Okumura and M. Shinji, eds., "Fundamentals of mobile communications" published in Japanese by IEICE, 1986; M. Shinji, ed., "Mobile communications" published in Japanese by Maruzen Publishing Co., 1989; and M. Kuwabara ed., "Digital mobile communications" published in Japanese by Kagaku Shinbun-sha, 1992. He was a co-recipient of the IEICE Transactions best paper of the year award 1996 and again 1998. He is an IEEE Fellow and was a co-recipient of the IEEE Vehicular Technology Transactions best paper of the year award 1980 and again 1990 and also a recipient of Avant Garde award 2000.